Egypt. J. Chem. **Vol. 66**, No. SI: 13 pp. 1621 - 1632 (2023)

Egyptian Journal of Chemistry

http://ejchem.journals.ekb.eg/

Evaluation of Gamma-Rays Attenuation Parameters of Novel Lead-Borate Glass System for Radiotherapy Room

Mona Abo Zeed[a], R. M. El Shazly[b] , H. M. El- Mallah[a] , E. Elesh[c], Aly Saeed[d*]

[a]*Mathematics and Physics Department, Faculty of Engineering, Port Said University, Egypt*

[b]*Department of Physics, Faculty of Science, Al-Azhar University, Egypt*

[c]*Department of Physics, Faculty of Science, Port Said University, Egypt Abstract*

[d]*Mathematical and Natural Science Department, Faculty of Engineering, Egyptian – Russian University, Egypt*

Abstract

The development of radiation therapy necessitated continuous research and development (R&D) for radiotherapy rooms' glass windows to reach the highest levels of protection for the staff of the radiotherapy facility. Therefore, in this article, a novel type of lead borate glass depending on the parallel augmenting of lead and boron simultaneously was produced to be used as gamma-rays and thermal neutrons barriers in radiotherapy rooms. Thermal neutrons and gamma rays' attenuation parameters, thermal neutron total cross section σ_T, mass attenuation coefficient σ, linear attenuation coefficient μ, half-value layer HVL, mean free path MFP, effective atomic number Z_{eff}, effective electron density N_{eff}, and buildup factor for energy absorption EABF and exposure EBF were studied extensively. Three tools, Phy-X/PSD, EpiXS, and XCOM computer programs as well as the standard mixture rules were utilized to estimate the attenuation parameters. A significant improvement in the gamma rays and thermal neutrons attenuation parameters was observed with the augmentation of lead and boron concentrations. A reduction in the HVL of the glass containing the highest concentration of Pb and B (40 mol% of Pb and 50 mol% of B) ranged between 42.425 and 97.761% for the studied gamma rays was observed, while the required HVL for thermal neutrons shrunk by 68.8%. Hence, the glass containing 40 mol% of Pb and 50 mol% of B was recommended to be a distinguished choice as a shield in the radiotherapy room.

Keywords: Radiotherapy room, Shielding materials, Lead-borate glass, Neutrons, Gamma rays

1. Introduction

Radiotherapy is one of the advanced methods of tumors diagnosis and treatment using neutrons, protons, and gamma ray sources [1-2]. In the radiotherapy room, the control console area or window for monitoring patient position must be shielded adequately from the primary, scatter, and leakage radiation. This is usually achieved through a leaded-glass window lined to allow a full view of the patient and the simulator for the gamma radiotherapy room [3-8]. While in the boron neutron capture therapy (BNCT) room, the shield must be inlaid by high thermal neutron cross section elements [3-8]. On the other hand, in gamma ray radiotherapy room, neutron contamination induced through photoneutron interaction of high energetic gamma ray, greater than 8 MeV, with barriers must be taken into consideration [9]. The abundance of electrons in lead as well as its ease of formation and addition made it the most common element as an efficient attenuator for gamma ray [10-13]. Light elements come first as the most efficient attenuator of fast neutrons through elastic collisions, then the heavy elements through inelastic collisions. For thermal neutrons, high cross-section elements such as B, Cd, and Gd must be added [14-16]. One of the critical criteria for the efficient neutrons' attenuator, fast and thermal, which must be taken into consideration is the secondary emission of gamma rays produced from the nuclear reactions of neutrons with that attenuator [14-16]. Whenever the neutrons' attenuator, fast or thermal, emits few and lower energies of gamma rays, the higher its efficiency [14-16]. The other criterion is it contains heavy metals to absorb the emitted secondary gamma-ray i.e., self-absorption [14-16]. In this regard, many researches were conducted to develop multicomponent glass materials with high vision and efficient ability to attenuate different

*Corresponding author e-mail: aly-saeed@eru.edu.eg; (Aly Saeed).

EJCHEM use only: Received date 19 May 2023; revised date 27 July 2023; accepted date 17 August 2023

DOI: 10.21608/EJCHEM.2023.212043.7997

nuclear radiation. In 2015, Mehdi Pouryavi studied the radiation shielding parameters for the Boron Neutron Capture Therapy (BNCT) room sectors, walls, monitoring window, maze, and entrance door. The authors concluded that their proposed design for BNCT is safe [4]. In their study, which was conducted in 2020 [17], Gurinder Pal Singh et al analyzed the gamma ray shielding ability of WO_3-Al_2O_3-PbO-B_2O_3 glass using Phy-X/PSD software. Accordingly, the authors concluded that the tungsten imparts a high attenuation ability to the glass, which enables it to be used as a shield against gamma rays. In 2020, G. Lakshminarayana et al [18] studied the attenuation parameters of (Bi_2O_3)x-(TeO_2)(100-x) and $[(TeO_2)_{0.7}$-$(B_2O_3)_{0.3}]$(1-x)-(Bi_2O_3)x glass using MCNP5 simulation code and WinXCom software. In their conclusion, the authors suggested the $49TeO_2$–$21B_2O_3$–$30Bi_2O_3$ (mol%) glass as the best attenuator for fast neutron, while that $66.5TeO_2$–$28.5B_2O_3$–$5Bi_2O_3$ (mol%) for thermal neutron. In 2022 [19], M. H. A. Mhareb et al studied the structural properties and gamma ray, neutrons, and charged particles attenuation ability of (70-x)TeO_2-xMoO_3-10SrO–20BaO. The authors found that the attenuation ability for gamma rays and neutrons improved with inlying MoO_3. In 2023 [20], M. Humaid et al used a solid waste containing PbO to produce a lead borosilicate glass system. They found that the produced glasses had a suitable transparency and their attenuation efficiency significantly improved with the increase of PbO concentrations.

Hence, the present article is focusing on the study of the attenuation properties of $(30 + \mathrm{x})\mathrm{B_2O_3} - (60 - 3\mathrm{x})\mathrm{Na_2O} - 10\mathrm{ZnO} - 2\mathrm{xPb_3O_4}$ glass, where $\mathrm{x} = 0, 5, 10, 15$, and 20 mol% using the Phy-X/PSD, EpiXS, and XCOM computer programs as well as the standard mixture rules. All the attenuation coefficients for gamma rays and thermal neutrons have been discussed in detail. The novelty of this study is based on increasing the concentrations of lead and boron simultaneously to achieve the optimal attenuation ability for gamma rays and thermal neutrons together and achieving the self-absorption of secondary gamma rays, which are generated as a result of the interaction of neutrons with glass constituents.

2. Experimental procedures

Highly transparent glasses of the chemical composition$(30 + x)B_2O_3 - (60 - 3x)Na_2O - 10ZnO - 2xPb_3O_4$, where $x = 0,5,10,15$,and 20 mol% were synthesized and prepared via the melt-quenching method according to **Figure 1**. The samples were encoded as PbB1, PbB2, PbB3, PbB4, and PbB5 for $x = 0,5,10,15$, and 20 mol% respectively. The pure raw materials of H_3BO_3, Na_2CO_3, ZnO, and Pb_3O_4 were weighted, mixed, and grind well to get a united color as an indicator of pre-homogeneity. The mixture was melted at 1050 °C and poured in a stainless-steel mold inside the annealing furnace at 340 °C for one hour. The furnace was then closed and the samples were allowed to cool down inside it. Then, highly transparent glasses as shown in **Figure 2** were obtained. The variation of the glass color with the increase in Pb_3O_4 concentrations arose as a result of the penetration of Pb^{2+} ions within the glass network. The density of the produced glasses PbB1, PbB2, PbB3, PbB4, and PbB5 are 2.661, 3.274, 3.886, 4.499, and 5.111 gm/cm^3 respectively. The structural, thermal, and optical properties of the considered glasses were extensively studied previously [21].

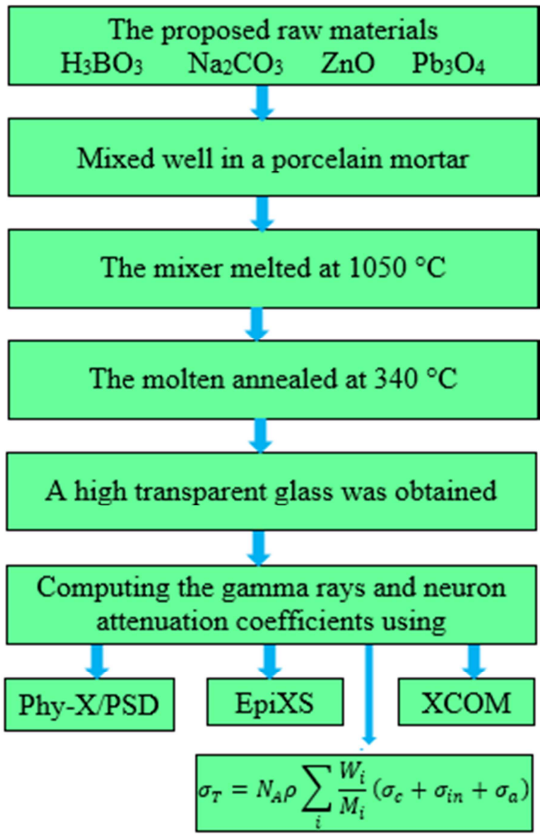

Figure 1: The schematic diagram of the fabrication process of the considered glasses

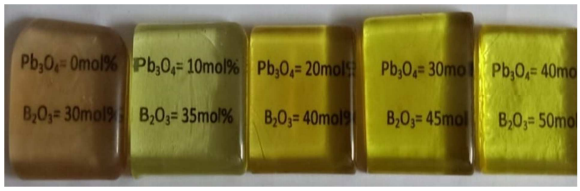

Figure 2: The high transparent fabricated glasses

Phy-X/PSD, EpiXS, and XCOM computer programs were used to study the effect of increased lead concentrations on the attenuation ability of gamma rays. The main algorithms of the used Phy-X/PSD and EpiXS softwares are extensively discussed by Erdem Şakar et al and Frederick C. Hila et al [22-26].

removal cross section of the i[th] constituents

For thermal neutron, the total macroscopic cross section was calculated using [18, 24]

$$\sigma_T = N_A \rho \sum_i \frac{W_i}{M_i} (\sigma_c + \sigma_{in} + \sigma_a) \qquad (2)$$

where, N_A, ρ, W_i, and M_i are the Avogadro's number, density, i[th] element mass fraction, and i[th] element atomic mass and $\sigma_c, \sigma_{in},$ and σ_a are the coherent scattering, incoherent scattering, and absorption cross sections of the thermal neutrons.

3. Results and discussion

The attenuation of gamma ray mainly depends on its energy and the chemical composition of the barrier. The photoelectric, Compton effect, and pair production interactions are the most probable interactions between gamma rays and the atomic structure of the protective materials. Accordingly, the behavior of the total mass attenuation coefficient σ of the studied glass, which showed in **Figure 3** and **Table 1** was discussed in detail. The total mass attenuation coefficient refers to the sum of the partial attenuation coefficients/partial cross sections of the three aforementioned interactions $= \tau/\rho + \sigma/\rho + \kappa/\rho$, where τ/ρ, σ/ρ, and κ/ρ are the cross sections of the photoelectric, Compton, and pair production interactions respectively. In Pb-free sample PbB1, mainly two different behaviors are observed in the studied gamma ray range from 1 keV to 100 GeV. A continuous, sharp and meager, reduction behavior in the σ is observed up to 26 MeV of gamma energy followed by slight growth in the rest of the studied gamma ray energies spectrum. In the low energy region up to 100 keV, the mass attenuation coefficients have the highest values due to the domination of the photoelectric effect interaction (the incident gamma photon interacts with the inner shell electrons and completely absorbed), which its cross section strong depends on the atomic number of the barrier Z, $\tau/\rho \propto Z^m$, where $m = 3.6 - 5.3$ [19, 27]. In this process, gamma photons are completely absorbed producing photoelectrons, which explains the high values of the σ in the lowest energies region. The observed sharpest diminution in σ with the increase of the gamma ray energy arose due to proportional of the photoelectric cross section τ/ρ with E^{-n}, where $n = 2.5 - 3.5$ [19, 27]. In the region up to 100 keV, the discontinuities (jumps) in the σ values around 1.043 and 1.194 keV are attributed to the absorption of gamma photons in L_2 and L_3-edges of Zn and that around 1.072 and 9.659 keV to K_1-edge of Na and K_1-edge of Zn. The meager diminution in σ in the zone from 100 keV to 26 MeV is attributed to the Compton effect (the incident gamma photon interacts with the outer shell electrons producing an electron and scattered gamma photon), in which its cross section σ/ρ is proportional to E^{-1} [19, 27]. Gamma photons' interaction through the Compton effect macerates the gamma-ray via incoherent scattering, producing a photon with weaker energy. So, in this region; the absorption of gamma photons occurs through two or more interactions, which reflects the reason for the decline values of the mass attenuation coefficient. Another reason for the low values of σ in this region is due to the weakly depends of its cross section on the atomic structure of the barrier constituents, $\sigma/\rho \propto Z$. In the second behavior; where the dominant here is the pair production interaction, as the gamma photons interact with the electrostatic field around the nucleus, a re-increase in the mass attenuation coefficients was observed due to the pair production cross section depends on Z^2, $\kappa/\rho \propto Z^2$[19, 27]. With lead insertion into the proposed glass, many changes occurred reflecting its effective role to attenuate gamma radiation. With lead insertion and its gradual augmentation, the limit of the sharpest region was shifted towards the higher gamma ray energy, 150, 200, and 300 keV for 10, 20, and 30 &40 mol% of Pb respectively. Also, new jumps arose at 2.484, 2.586, 3.066, 3.544, and 3.581 keV, which attributed to the gamma photons interactions with M_1, M_2, M_3, M_4, and M_5 edges of Pb respectively. While, the jumps at 13.04, 15.2, and 15.86 keV attributed to the interactions with L_1, L_2, and L_3 edges, and that at 88 keV to K-edge of Pb. All the observed edges were shifted towards the high gamma ray energy with the increase of Pb concentrations. On the other hand, the beginning of the pair production interaction differed significantly with the increase of Pb concentrations, 28, 20, 14, and 10 MeV at 0, 10, 20, and 30 &40 mol % of Pb respectively. The shift of the beginning of the pair production interaction region towards the low energy is attributed to the increase of the density of the electrostatic field of the medium with the increase in lead concentrations. The gradual shift of mass attenuation coefficients in the photoelectric effect

region to the higher energy reaching up to 300 keV and the lower energy shift in pair production up to 10 MeV, which means the photoelectric effect and pair production cover wide ranges of gamma ray energies, indicates that Pb reinforced the glass ability to attenuate gamma ray. The enhancement of the attenuation ability of the glass arose due to its crowding with electrons, resulting from the increase of lead (Z=82) atoms.

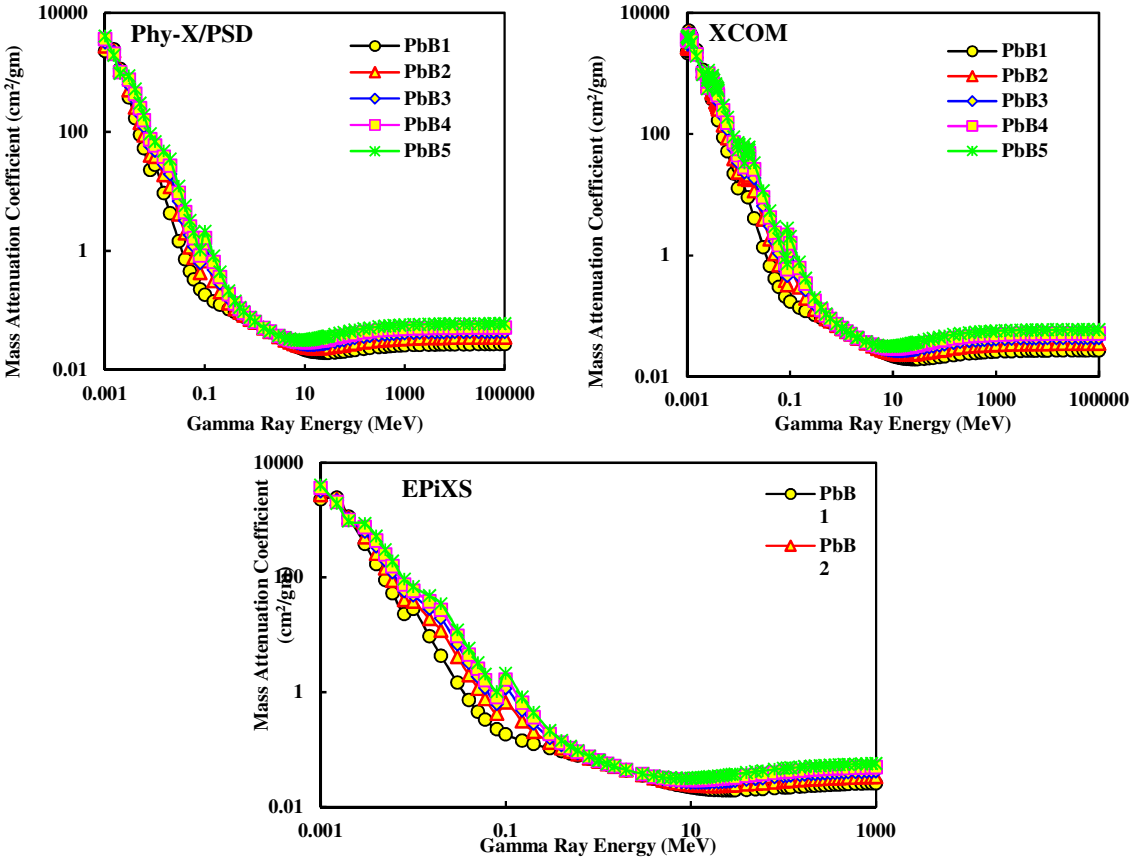

Figure 3: Mass attenuation coefficients of the studied glasses as a function in gamma ray energy in the range of 1 keV up to 10^4 MeV using Phy-X/PSD, EpiXS, and XCOM softwares

Table 1: Variation of mass attenuation coefficients with Pb concentrations

Energy Range	Energy (MeV)	Phy-X/PSD					XCOM					EPiXS				
		PbB1	PbB2	PbB3	PbB4	PbB5	PbB1	PbB2	PbB3	PbB4	PbB5	PbB1	PbB2	PbB3	PbB4	PbB5
Low	0.1	0.183	0.671	1.159	1.648	2.136	0.172	0.642	1.112	1.582	2.053	0.183	0.671	1.160	1.648	2.137
	0.2	0.124	0.204	0.283	0.363	0.442	0.121	0.195	0.270	0.344	0.418	0.124	0.204	0.284	0.3634	0.443
	0.3	0.105	0.132	0.159	0.187	0.214	0.104	0.128	0.153	0.178	0.202	0.105	0.132	0.159	0.186	0.214
	0.5	0.085	0.092	0.099	0.106	0.113	0.084	0.090	0.096	0.102	0.109	0.085	0.092	0.099	0.106	0.113
Intermediate	1	0.062	0.063	0.063	0.064	0.065	0.062	0.062	0.063	0.063	0.064	0.062	0.063	0.063	0.064	0.065
	5	0.028	0.029	0.030	0.032	0.033	0.028	0.029	0.030	0.032	0.033	0.028	0.029	0.030	0.032	0.033
	10	0.022	0.024	0.027	0.029	0.032	0.022	0.024	0.027	0.029	0.032	0.022	0.024	0.027	0.029	0.032
	20	0.020	0.023	0.027	0.031	0.035	0.020	0.023	0.027	0.031	0.035	0.020	0.023	0.027	0.031	0.035
High	50	0.020	0.025	0.031	0.036	0.041	0.020	0.025	0.031	0.036	0.041	0.020	0.025	0.031	0.036	0.041
	100	0.022	0.028	0.034	0.040	0.047	0.022	0.028	0.034	0.040	0.047	0.022	0.028	0.034	0.040	0.047
	500	0.025	0.032	0.040	0.048	0.055	0.025	0.032	0.040	0.048	0.055	0.025	0.032	0.040	0.048	0.055
	10000	0.027	0.035	0.043	0.051	0.059	0.026	0.034	0.041	0.049	0.057	0.026	0.034	0.041	0.049	0.057
	100000	0.027	0.035	0.043	0.052	0.060	0.027	0.035	0.043	0.052	0.060	–	–	–	–	–

Concerning to the dependency of the three processes of gamma rays interaction on the atomic number of the medium $\tau/\rho, \sigma/\rho, and\ \kappa/\rho \propto Z^m$, $Z, and\ Z^2$ respectively [19, 27] and as a comparison between the Pb-free sample and the gradation of lead increase, various energies of gamma rays in the low 0.1, 0.2, 0.3, and 0.5 MeV, intermediate 1, 5, 10, and 20 MeV, and high 50, 100, 500, 1000, and 10000 MeV regions are selected to study the effect of Pb-concentration on the attenuation ability of the considered glass as listed in **Table 1**.

It was found that the augmentation of Pb grants a strong improvement in the mass attenuation coefficient in low and high energy. While, in the intermediate energy a meager growth in mass attenuation coefficient was observed with Pb-concentration increase. The significant increment in the mass attenuation coefficients in the low and high energy regions with the increase of lead concentrations was attributed to the strong dependence of the cross-section in these two regions on atomic number, $\tau/\rho \propto Z^{3.6-5.3}$ for low energy and $\kappa/\rho \propto Z^2$ for high energy. On the other hand, the little variation in the intermediate region due to weak-dependent of cross section on Z, $\sigma/\rho \propto$ Z. The relative difference between Phy-X/PSD and EPiXS ranged from -0.406 to 0.3 %, Phy-X/PSD and XCOM from -0.016 to 8.305%, and EPiXS and XCOM from -1.405 to 9.747%. The strong convergence between the obtained results from the three programs confirms their validity and supports the validity of the used programs. The linear attenuation coefficient μ values as depicted in **Figure 4** showed the same manner of the mass attenuation coefficients. The highest density glass sample 40 mol% of Pb ($\rho = 5.111$ gm/cm^3) had the highest linear attenuation coefficient for all energies as shown in the inset of **Figure 3**.

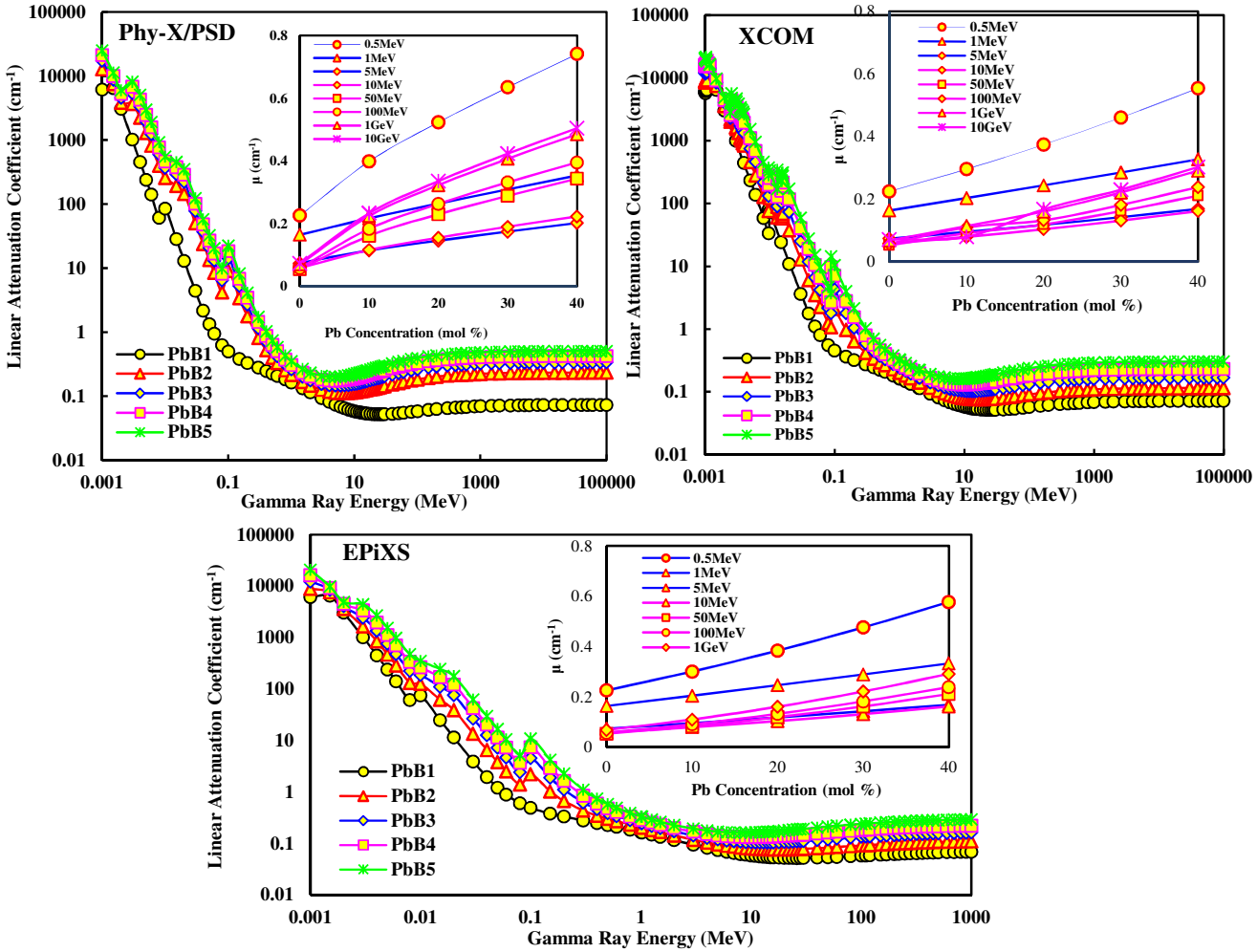

Figure 4: Variation of linear attenuation coefficients of the studied glasses obtained by Phy-X/PSD, EpiXS, and XCOM softwares as a function in photon energy in the range of 1 keV up to 10^4 MeV and Pb-concentration

The more interesting parameter in shielding design, Half Value Layer HVL is shown in **Figure 5**. HVL values raised with energy augmentation up to 26 MeV and return to decrease thereafter up to the end of the studied energy range. In the low energy region, in which the photoelectric effect is dominant, the strong decline in the HVL values is due to the high cross section of gamma ray interaction. In the intermediate region, the Compton region, the high values of HVL reflect a reduction in interaction probability leading to more penetration of gamma ray in this region. the re-decrease in HVL in the high energy region, the pair production region, arises due to the high interaction probability of gamma rays with the electrostatic field around the nucleus. In the photoelectric effect and pair production regions, it was found that the HVL strongly depends on the lead concentration as shown in the inset of **Figure 5**. It is observed that the HVL values decreased by Pb-increased until the highest Pb concentration insertion in the studied base glass network, which is the least of HVL and therefore the best as a shield.

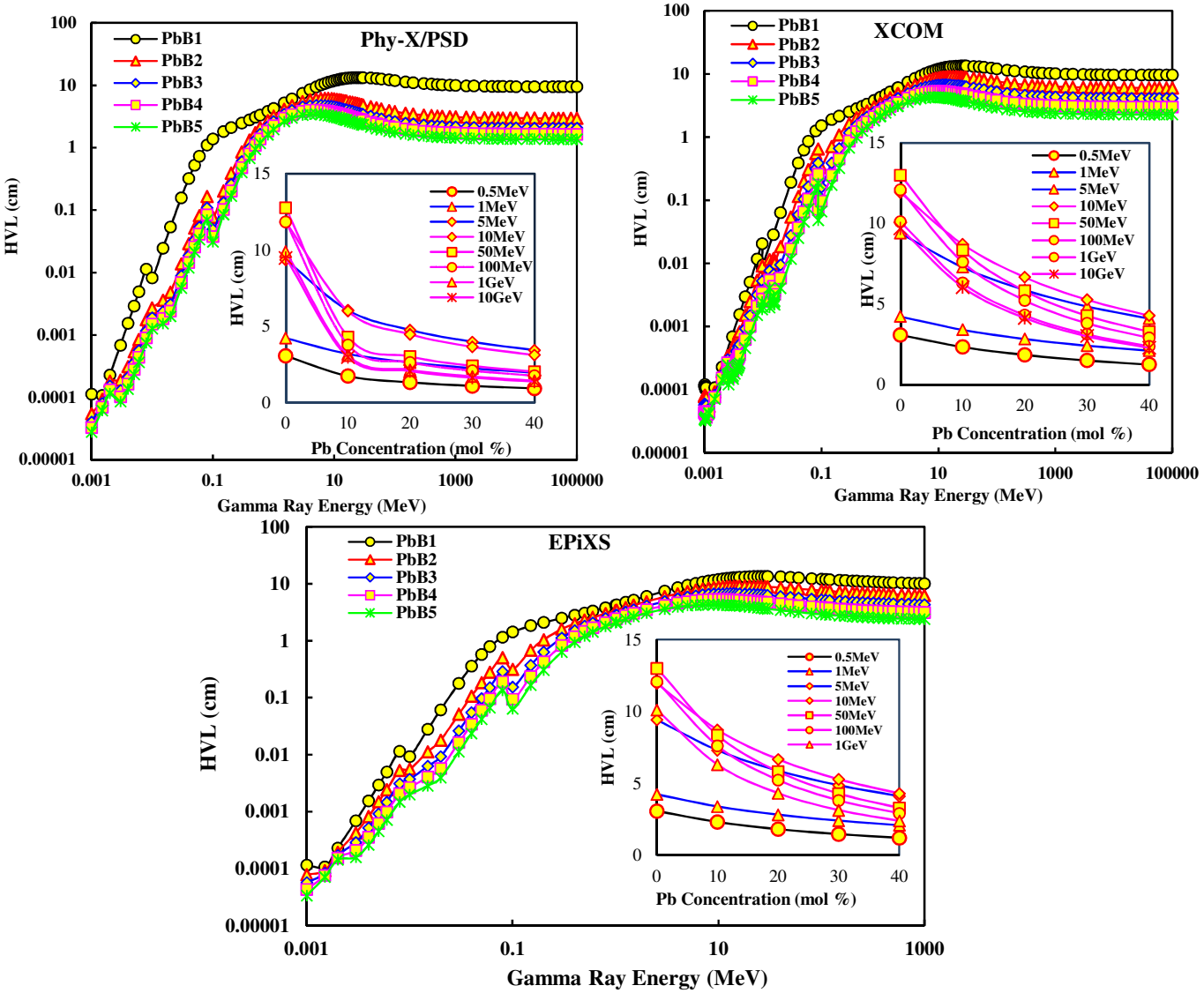

Figure 5: HVL of the investigated glass as a function in gamma ray energy in the range of 1 keV up to 10^4 MeV and Pb concentrations

Mean free path MFP as a function in gamma ray energy and in Pb-concentration is shown in **Figure 6**. It is well known that the MFP is inversely proportional to the linear attenuation coefficient, therefore it is found that the MFP values increase with the gamma-ray energy increase. The augmentation of the gamma-ray interaction probability with the studied barriers was accentuated through the decrease of the MFP values with the

increase of Pb-concentrations as shown in the inset of **Figure 6**.

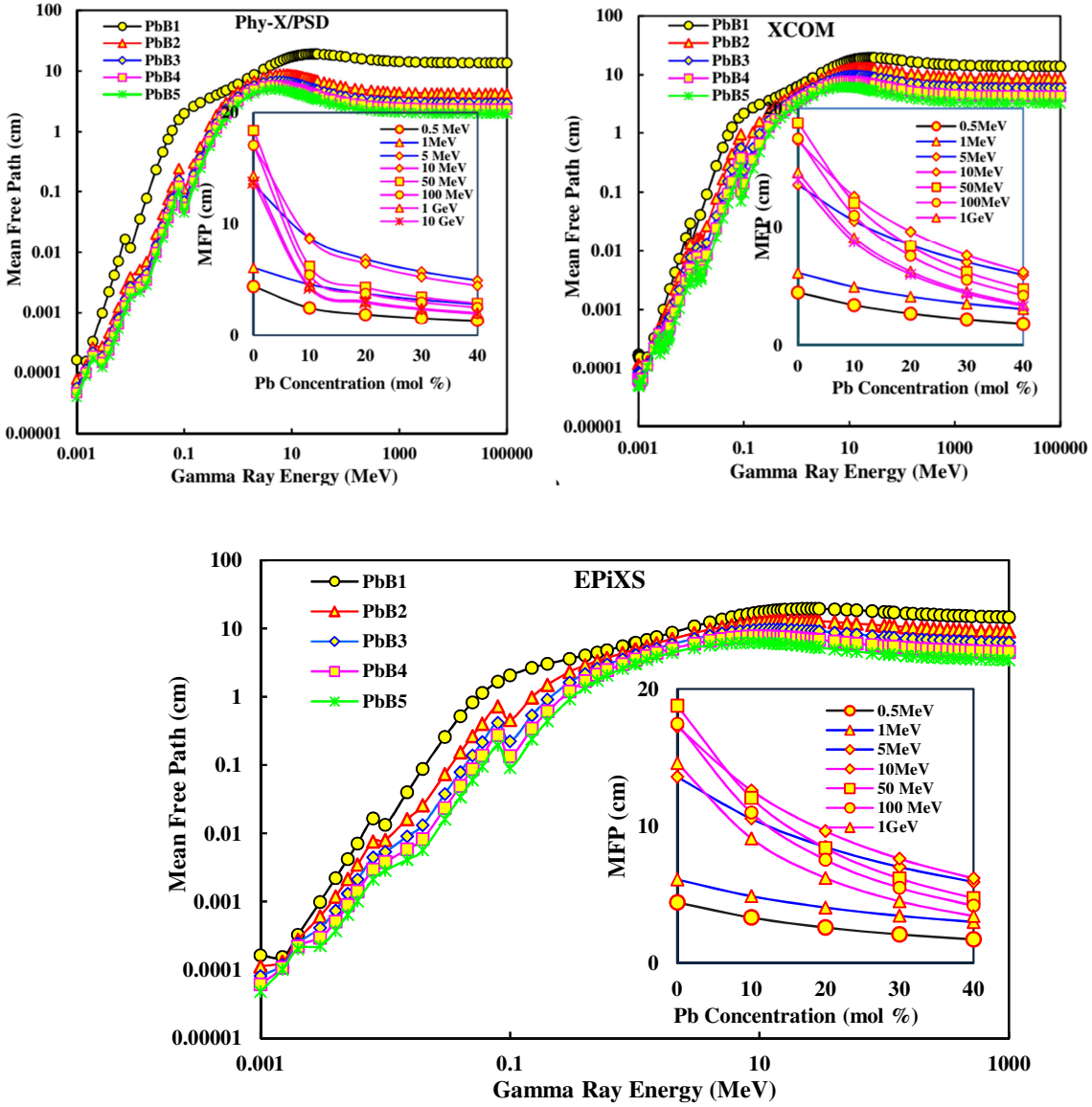

Figure 6: Mean free path of the studied glasses as a function in both photon energy in the range of 1 keV up to 10^4 MeV and Pb-concentration

The role of chemical composition (electronic density) is clearly shown in the attenuation of gamma ray through a study of the effective atomic number Z_{eff} and the effective electron density N_{eff}. The obtained results of both of them are shown in **Figure 7** and **8**. The highest values of Z_{eff} and N_{eff} were observed at low gamma energies followed by the highly energetic due to the gamma photons' interaction dependency on the atomic number. As mentioned previously, in low energy zone (photoelectric effect region) $E \propto Z^{3.6-5.3}$, while for the high energy (pair production region) $E \propto Z^2$. On the other hand, in the intermediate region (the Compton region); both of Z_{eff} and N_{eff} have the lowest values due to $E \propto$ Z. As shown in **Figures 7b** and **8b**, Pb has a strong effect on the attenuating ability of gamma rays, which both of Z_{eff} and N_{eff} showed a sonorous dependence on Pb concentrations. The highest values of Z_{eff} and N_{eff} were observed at low gamma energies followed by the highly energetic due to the gamma photons' interaction dependency on the atomic number. As mentioned previously, in low energy zone (photoelectric effect region) $E \propto Z^{3.6-5.3}$, while for the high energy (pair production region) $E \propto Z^2$. On the other hand, in the intermediate region (the Compton region); both of Z_{eff} and N_{eff} have the lowest values due to $E \propto$ Z. As shown in **Figures 7b** and **8b**, Pb has a strong

effect on the attenuating ability of gamma rays, which both of Z_{eff} and N_{eff} showed a sonorous dependence on Pb concentrations.

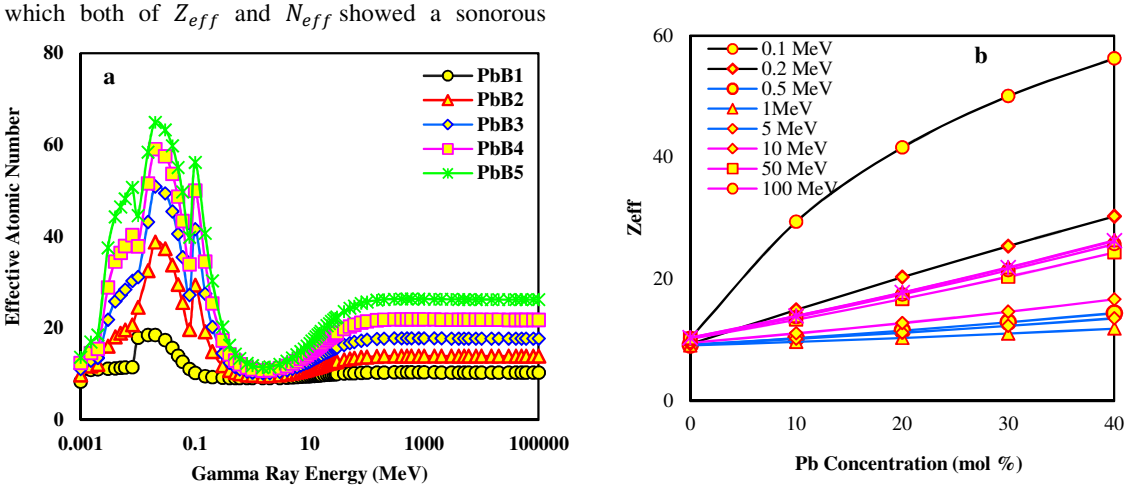

Figure 7: Effective atomic number as a function in a) photon energy in the range of 1 keV up to 10^4 MeV and b) Pb concentrations

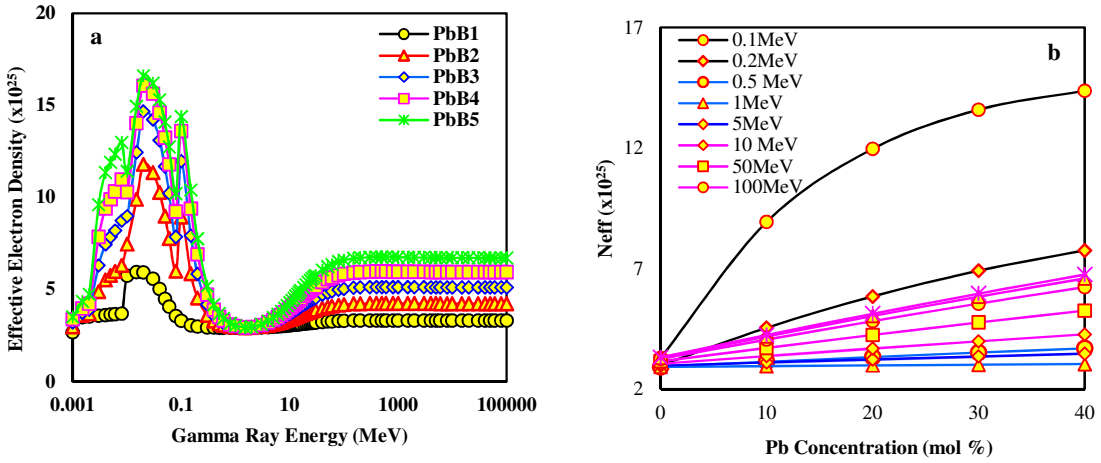

Figure 8: Effective electron density as a function in a) photon energy and b) Pb concentrations

In the lead-free sample, as shown in **Figure 9** and **10** it was observed that the Exposure Build-up Factor EBFs and Energy Absorption Buildup Factors EABFs increased with the increase of the photon energy until it reaches a peak at 0.3 MeV and decrease thereafter. It is known that the photoelectric effect process removes the energy of the photon when it interacts with the medium and thus prevents its accumulation inside the barrier. Hence, at low energies where the photoelectric interaction dominates; the least values of the EBFs and EABFs were observed. In the following region, where the Compton scattering is predominant, multiple scattering in gamma photons occurs leading to an increase in the EBFs and EABFs to reach their maximum value. A monotonous increase in the EBFs and EABFs was observed with the increase of the MFP, which was attributed to the increase in the incidence of the scattering, which resulted from the increase in the path traveled by the photon. The longer the path that the photon travels, the more scattering as a result of interaction with the medium constituents. It was also observed with the beginning of lead insertion and its increase, a decrease in the build-up factor was happened, which is attributed to a raise of equivalent atomic number. Lead penetration increases the probability of photon absorption into the medium, which reduces the scatterings.

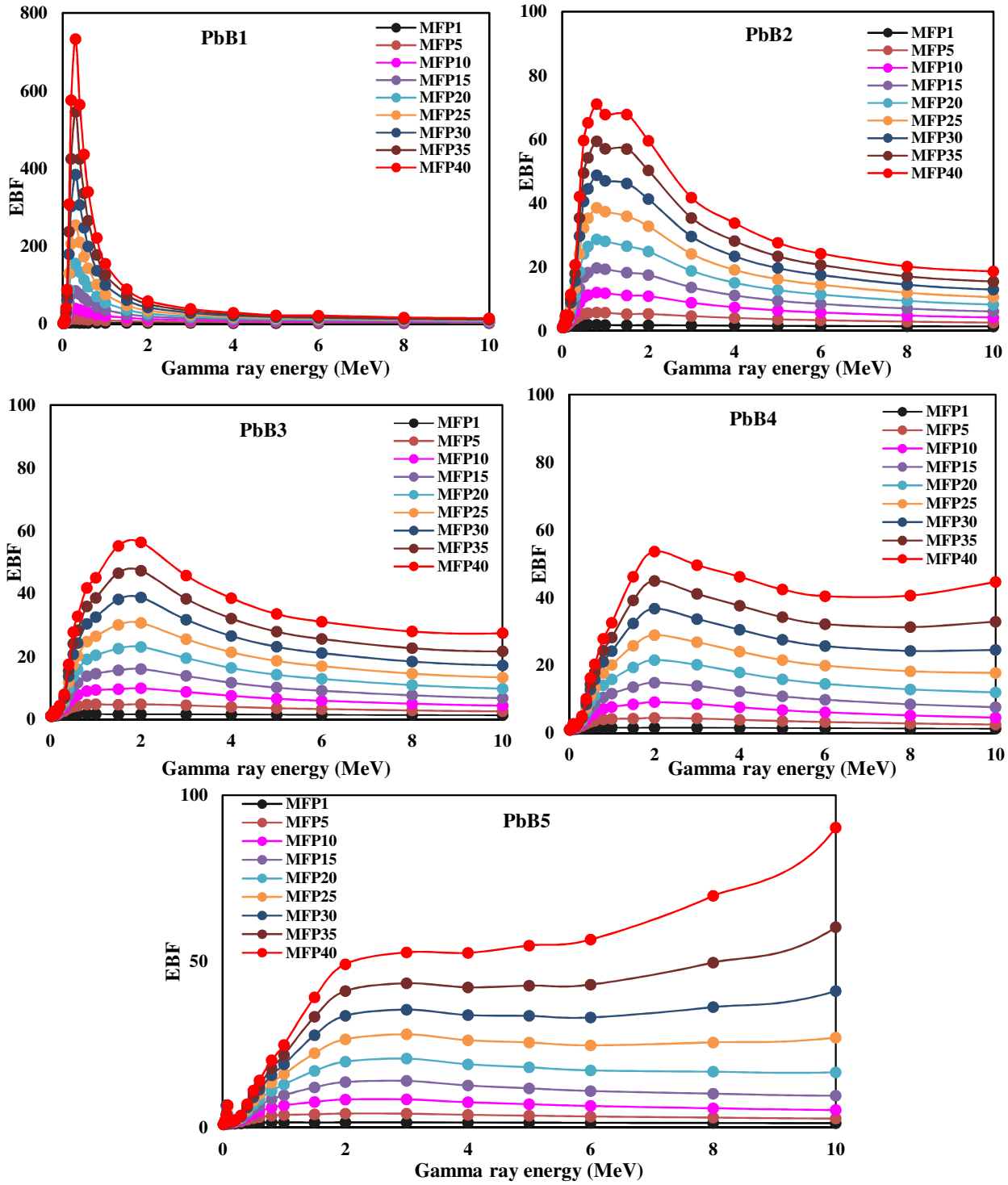

Figure 9: Exposure buildup factors for different MFP

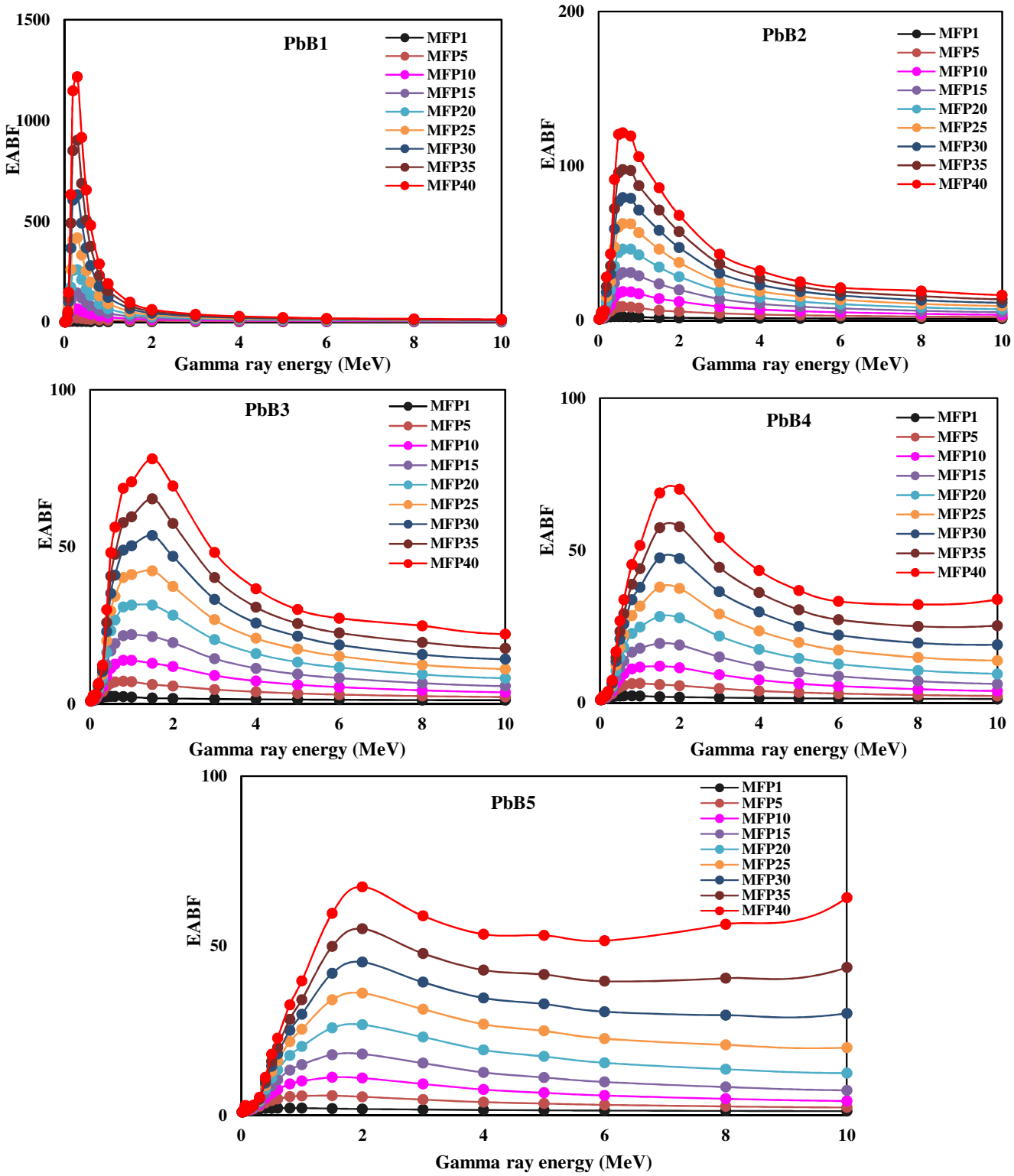

Figure 10: Energy absorption buildup factors as a function in photon energy

As a function of the boron concentration, the highest cross-section element for thermal neutrons in the considered glasses, the total cross-section of the thermal neutron is shown in **Figure 11**. The

significant increase in the cross-section was attributed to the increase in boron concentration.

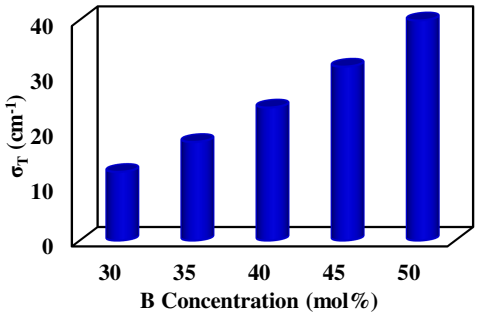

Figure 11: Thermal neutron cross section for the considered glasses

Conclusions

Five grades of highly transparent glasses PbB1 (30 and 0 mol% of B_2O_3 and Pb_3O_4), PbB2 (35 and 10 mol% of B_2O_3 and Pb_3O_4), PbB3 (40 and 20 mol% of B_2O_3 and Pb_3O_4), PbB4 (45 and 30 mol% of B_2O_3 and Pb_3O_4), and PbB5 (50 and 40 mol% of B_2O_3 and Pb_3O_4) were prepared and their attenuating properties were extensively studied to be used as shielding materials in radiotherapy rooms. Pb, the highest atomic number in the studied glass has a strong influence on the attenuating ability of all the studied gamma ray energies. A significant increase in the mass and linear attenuation coefficients and reduction in the required half value layers were observed with the increase of Pb concentrations. The HVL, the most interesting parameter in shielding design was reduced by a percentage ranging from 42.425 up to 97.761 for the studied gamma rays' energies. Given that its cross-section area for thermal neutrons is the highest, the boron has enhanced the ability of the considered glass to attenuate thermal neutrons. In PbB5 glass, the required HVL for thermal neutrons was reduced by 68.8%. According to the results of this study, the considered PbB5 glass (contains 40 mol% of Pb and 50 mol% of B) is a strong candidate for use in radiotherapy room designs.

Reference

1. Afkham,Younes, Mesbahi, Asghar, Alemi, Abdolali, Zolfagharpour, Farhad, and Jabbari, Nasrollah, Design and fabrication of a nano-based neutron shield for fast neutrons from medical linear accelerators in radiation therapy. Radiation Oncology, 15, 1-13 (2020).
2. Han, Gaoab, Long, Chenc, Tang, Bo, Wang, Yidi, Du, Chuansheng, Liu, Kun, Qiu, Dong, Kong, Xianghui, Yang, Bing, Yin, Yuchen, Zhang, Wenyue, Tu, Yu, and Sun, Liang, Calculation of shielding performance of CRT concrete for proton therapy and optimal shielding design of treatment delivery room. Applied Radiation and Isotopes, 189, 110432 (2022).
3. Afrianti, E., Tahir, D., Jumpeno, B. Y. E. B., Firmansyah, O. A., Mellawati, J., Addition of lead (Pb)-nitrate filler on polymer composite aprons for X-ray radiation shielding, Atom Indonesia, 47(2), 129 – 133 (2021).
4. Chen, Jun-Yang, Tong, Jian-Fei, Hu, Zhi-Liang, Han, Xue-Fen, Tang, Bin, Yu, Qian, Zhang, Rui-Qiang, Zhao, Chong-Guang, Xu, Jun, Fu, Shi-Nian, Zhou, Bin and Liang, Tian-Jiao, Evaluation of neutron beam characteristics for D-BNCT01 facility. Nuclear Science and Techniques, 33, 12 (2022).
5. Fetterly, Kenneth A., Magnuson, Dixon J., Tannahill, Gordon M., Hindal, Mark D., and Mathew, Verghese, Effective use of radiation shields to minimize operator dose during invasive cardiology procedures. JACC: Cardiovascular Interventions, 4 (10), 1133-1139 (2011).
6. Hu, Naonori, Tanaka, Hiroki, Kakino, Ryo, Yoshikawa, Syuushi, Miyao, Mamoru, Akita, Kazuhiko, Isohashi, Kayako, Aihara, Teruhito, Nihei, Keiji, and Ono, Koji, Evaluation of a treatment planning system developed for clinical boron neutron capture therapy and validation against an independent Monte Carlo dose calculation system. Radiation Oncology 16, 1-13 (2021).
7. Adeniji, A. R., Ezema, I. C., Aderonmu, P. A., and Adesipo, A. O., Radiation protection strategies in medical diagnostic centers in Lagos State, Nigeria. IOP Conf. Series: Materials Science and Engineering 640, 1-17 (2019).
8. Aygün, B., Yorgun, N. Yıldız, Sayyed, N. I., Karabulut, A., $Li_2B_4O_7$–Bi_2O_3–ZrO_4–$CaWO_4$ glass system for neutron protection in neutron applications. Progress in Nuclear Energy 162, 104751 (2023).
9. Saeed, Aly, Elbashar, Y. H., and El Kameesy, S. U., Study of gamma ray attenuation of high-density bismuth silicate glass for shielding applications. Research Journal of Pharmaceutical, Biological and Chemical Sciences, 6(4), 1830 – 1837 (2015).
10. Saeed, Aly, Elbashar, Y. H., and El Kameesy, S. U., Optical spectroscopic analysis of high density lead borosilicate glasses. Silicon, 10, 185 – 189 (2018).
11. Saeed, Aly, Elbashar, Y. H., and El Kameesy, S. U., A novel barium borate glasses for optical applications. Silicon, 10, 569–574 (2018).
12. Saeed, Aly, Elbashar, Y. H., and El shazly, R. M., Optical properties of high density barium borate glass for gamma ray shielding applications. Optical and Quantum Electronics, 48(1) 1-10 (2016).
13. Saeed, Aly Abdallah, El Shazly, Raed Mohamed, El-Okr, Mohamed Mahmoud, Abou El-Azm, Ali Moheeb, Elbashar, Yahia Hamdy, Comsan, Mohamed Nasef Hassan, Kansouh, Wagdy Ahmed, and El-Sersy, Ahmed Reda, Neutron shielding properties of a borated high-density glass", Nuclear Technology & Radiation Protection. 32 (2), 120-126 (2017).
14. Saeed, Aly, El shazly, R. M., Elbashar, Y. H., Abou El-azm, A. M., Comsan, M. N. H., El-Okr,

M. M., and Kansouh, W. A., Glass materials in nuclear technology for gamma ray and neutron radiation shielding: a review. Nonlinear Optics, Quantum Optics, 53, 107–159 (2020).
15. El-kameesy, S. U., Eissa, M. M., El-Fiki, S. A., El Shazly, R. M., Ghalib, S. N., and Saeed, A., A Phenomenological study on the gamma rays attenuation properties of developed steel alloys. Arab Journal of Nuclear Science and Applications, 50 (1), 1-9 (2017).
16. Saeed, Aly, El shazly, R. M., Elbashar, Y. H., Abou El-azm, El-Okr, M. M., A. M., Comsan, M. N. H., Osman, A. M., Abdal-monem, A. M., and El-Sersy, A. R., Gamma ray attenuation in a developed borate glassy system. Radiation Physics and Chemistry 102, 167–170 (2014).
17. Singh, Gurinder Pal, Singh, Joga, Kaur, Parvinder, Kaur, Simranpreet, Arora, Deepawali, Kaur, Ravneet, Kaur, Kulwinder, and Singh, D. P., Analysis of enhancement in gamma ray shielding proficiency by adding WO_3 in Al_2O_3-PbO-B_2O_3 glasses using Phy-X/PSD", Journal of Materials Research and Technology. 9, 14425-14442 (2020).
18. Lakshminarayana, G., Kebaili, Imen, Dong, M. G., Al-Buriahi, M. S., Dahshan, A., Kityk, I. V., Lee, Dong-Eun, Yoon, Jonghun, and Park, Taejoon, Estimation of gamma-rays, and fast and the thermal neutrons attenuation characteristics for bismuth tellurite and bismuth boro-tellurite glass systems. Journal of Materials Science 55, 5750–5771 (2020).
19. Mhareba, M. H. A., Sayyed, M. I., Hashim, S., Alshammari, Maha, Alhugail, Shadin, Aldoukhi, Houra, Hamad, M. Kh, Alajerami, Y. S., and Khandaker, Mayeen Uddin, Radiation shielding features for a new glass system based on tellurite oxide. Radiation Physics and Chemistry, 200, 110094 (2022).
20. Humaid, M., Asad, J., Aboalatta, A., Shaat, S. K. K., Musleh, H., Ramadan, Kh., Alajerami, Y., Aldahoudi, N., Gamma and neutron shielding properties of lead-borosilicate shielded glass; novel technique of solid waste recycling. Construction and Building Materials 375, 130896 (2023).
21. Abo Zeed, Mona, Saeed, Aly, El Shazly, R. M., El- Mallah, H. M., Elesh, E., Double effect of glass former B_2O_3 and intermediate Pb_3O_4 augmentation on the structural, thermal, and optical properties of borate network. Optik 272, 170368 (2023).
22. Şakar, Erdem, Özpolat, Özgür Fırat, Alım, Bünyamin, Sayyed, M.I., Kurudireka, Murat, Phy-X / PSD: Development of a user friendly online software for calculation of parameters relevant to radiation shielding and dosimetry. Radiation Physics and Chemistry 166, 108496 (2020).
23. Hila, Frederick C., Astronomo, Alvie Asuncion, Dingle, Cheri Anne M., Jecong, Julius Federico M., Hila, Abigaile Mia V. Javier, Gili, Mon Bryan Z., Balderas, Charlotte V., Lopez, Girlie Eunice P., Guillermo, Neil Raymund D., Jr., Alberto V. Amorsolo, EpiXS: A Windows-based program for photon attenuation, dosimetry and shielding based on EPICS2017 (ENDF/B-VIII) and EPDL97 (ENDF/B-VI.8). Radiation Physics and Chemistry 182, 109331(2021).
Zaid, M. H. M., Matori, K. A., Sidek, H. A. A., Ibrahim, I. R., Shielding characteristics of nanocomposites for protection against X- and gamma rays in medical applications: effect of particle size, photon energy and nano-particle concentration. Radiation and Environmental Biophysics 59, 583-600 (2020).
24. Osman, A. M.,Calculation of gamma and neutron shielding parameters for reinforced polymer composites. Journal of Nuclear Engineering and Radiation Science 9(1), 012002 (2023).
25. Mhareb, M. H. A., Alajerami, Y. S. M., Dwaikat, Nidal, Al-Buriahi, M. S., Alqahtani, Muna, Alshahri, Fatimh, Saleh, Noha, Alonizan, N., Saleh, M. A., and Sayyed, M. I., "*Investigation of photon, neutron and proton shielding features of H_3BO_3-ZnO-Na_2O-BaO glass system*", Nuclear Engineering and Technology, 52, 949-959 (2021).
26. Teresa, P. Evangelin, Naseer, K. A., Marimuthu, K., Alavian, Hoda, and Sayyed, M. I., "Influence of modifiers on the physical, structural, elastic and radiation shielding competence of Dy^{3+} ions doped Alkali boro-tellurite glasses", Radiation Physics and Chemistry 189, 109741 (2021).